arXiv:cond-mat/0405658v1 [cond-mat.stat-mech] 27 May 2004

Rotating Bose-Einstein condensates with attractive interactions

G. M. Kavoulakis,[1] A. D. Jackson,[2] and Gordon Baym[3,4]
[1] *Mathematical Physics, Lund Institute of Technology, P. O. Box 118, S-22100 Lund, Sweden*
[2] *Niels Bohr Institute, Blegdamsvej 17, DK-2100 Copenhagen Ø, Denmark*
[3] *Department of Physics, University of Illinois at Urbana-Champaign, 1110 West Green Street, Urbana, Illinois 61801*
[4] *NORDITA, Blegdamsvej 17, DK-2100 Copenhagen Ø, Denmark*
(Dated: March 22, 2022)

We examine the phase diagram of a Bose-Einstein condensate of atoms, interacting with an attractive pseudopotential, in a quadratic-plus-quartic potential trap rotating at a given rate. Investigating the behavior of the gas as a function of interaction strength and rotational frequency of the trap, we find that the phase diagram has three distinct phases, one with vortex excitation, one with center of mass excitation, and an unstable phase in which the gas collapses.

PACS numbers: PACS numbers: 03.75.Hh, 03.75.Kk, 67.40.Vs

I. INTRODUCTION

The velocity field of a superfluid is irrotational. As a result, such fluids develop vortex states when rotated, and the circulation of the superfluid velocity around any closed path is quantized [1]. Trapped Bose-Einstein condensates of alkali-metal atoms provide ideal systems for testing these ideas. Remarkably, they permit experimentalists not only to vary the form of the trapping potential but also to change the sign of the scattering length associated with the effective atom-atom interaction.

In a harmonic trap, vortices in Bose-Einstein condensates with repulsive interactions are always singly-quantized [2, 3]. If, however, the effective interaction is attractive or the trapping potential has a different shape [4], the situation can change dramatically. The recent experiment of Ref. [4] investigated the behavior under rotation of an effectively repulsive Bose-Einstein condensate confined in an anharmonic trap. As shown in the theoretical studies of Refs. [5, 6, 7, 8, 9, 10, 11, 12], vortices can be multiply quantized in any trap that grows faster than quadratically. Further, Refs. [13, 14, 15] have demonstrated that the angular momentum is carried by center-of-mass motion in an effectively-attractive condensate that rotates in a harmonic trap.

In this study we investigate the phase diagram of an anharmonically-trapped Bose gas in the case of an effective attractive atomic interaction as a function of the rotation frequency of the trap and of the strength of the dimensionless coupling constant, Na/Z, where N is the total number of atoms, a is the s-wave scattering length, and Z is height of the gas along the rotation axis. Both the sign and the magnitude of the scattering length can be adjusted using Feshbach resonances. The magnitude of the coupling constant can also be controlled by changing either the number of atoms in the trap or the trap frequencies. For sufficiently strong attractive interactions, such systems are unstable against collapse [16, 17, 18]. However, as long as the interaction is balanced by the zero-point motion of the atoms in the trap (and also by the kinetic energy associated with the vortices in the case of a rotating gas), the gas can exist in a metastable state.

In discussing the effects of rotation on the metastability of a gas with attractive interactions we must distinguish two physical situations, whether the trap is being rotated at a given angular frequency – the principal case we consider here – or whether the gas is set into rotation, and then the rotation of the trap is switched off. The former case, the analog of the Meissner effect in superconductors, examines the equilibrium states of the system in the presence of rotation. The latter examines the metastability of supercurrents in the absence of a driving force. As stressed by Leggett [19], superfluid flow in a system with effectively attractive interactions is not stable in the absence of external rotation. Thus the rotating states that we find here to be metastable in a rotating trap should lose angular momentum and cease rotating once the rotation of the trap is switched off. The details of how the angular momentum associated with superfluid flow in such systems is lost is beyond the scope of this paper. Examples of the breakup of a vortex are given in Refs. [20, 21]. Angular momentum can also be continuously taken out of the flow through interaction of the flow with normal fluid.

Anharmonic traps allow a rich structure of three phases depending on the strength of the attractive interactions and on the rotational frequency. The first is an unstable phase in which the gas collapses to a more dense state. The second phase is characterized by the angular momentum being carried by the motion of the center of mass. The third phase involves either a mixed state of multiply and singly quantized vortices or a pure state of multiple quantization. The general structure of the corresponding phase diagram is shown schematically in Fig. 1. References [22] have investigated this problem using both variational and exact numerical techniques. It is crucial that the trap be anharmonic to have such a structure. In a harmonic trap, repulsive interactions ensure that the critical frequency for rotation is smaller than the trap frequency and thus permit the formation of vortices [2]. Attractive interactions increase the critical frequency for rotation to a value larger than the trap frequency with the result that the centifugal force cannot be balanced by the restoring force of the trap and the atoms fly apart.

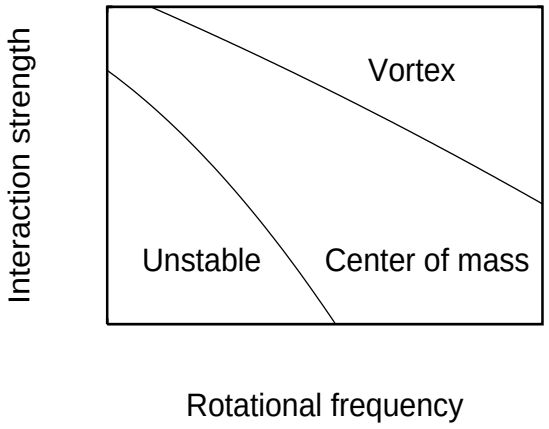


FIG. 1: Schematic phase diagram of a rotating Bose-Einstein condensate trapped in an anharmonic potential. The origin is the upper left corner. The vertical axis is the strength of the attractive effective atom-atom coupling constant and the horizontal axis is the rotational frequency of the trap.

In analyzing the problem we consider atoms interacting via a short-range effective interaction,

$$V_{\rm int} = \frac{1}{2} U_0 \sum_{i \neq j} \delta(\mathbf{r}_i - \mathbf{r}_j). \tag{1}$$

Here, $U_0 = 4\pi\hbar^2 a/M$ is the strength of the effective two-body interaction, where M is the atomic mass. We consider an anharmonic trapping potential of the form

$$V(\rho, z) = \frac{1}{2} M\omega^2 \rho^2 \left[1 + \lambda \left(\frac{\rho}{d_0} \right)^2 \right] + V_z(z). \tag{2}$$

Here, ω is the trap frequency of the harmonic potential perpendicular to the z axis (which is assumed to be the axis of rotation) and $d_0 = (\hbar/M\omega)^{1/2}$ is the oscillator length. The dimensionless constant λ is small (e.g., $\lambda \approx 5 \times 10^{-3}$ in the experiment of Ref. [4]) and V_z is the trapping potential along the z axis. Denoting the excitation energy of the first excited state along the z axis by ΔE_z, we assume that

$$n U_0 \ll \hbar\omega \ll \Delta E_z, \tag{3}$$

where n is the typical atom density. The inequality between the left and the right terms implies that the cloud is in its lowest state of motion along the z axis, and the problem thus becomes effectively two dimensional. Furthermore, under the above conditions, the typical density is $\sim N/d_0^2 Z$. The interaction energy nU_0 is $\sim \sigma a \hbar\omega$, where $\sigma = N/Z$ is the atom density per unit length. The assumption of small nU_0 in the left inequality of Eq. (3), is equivalent to $\sigma a \ll 1$.

In the following section, we examine the phase where the rotating gas forms vortices. In Sec. III we study the phase in which the angular momentum is carried by the center of mass, and in Sec. IV examine the unstable phase. Section V discusses the general features of the phase diagram, and Sec. VI summarizes our conclusions.

II. VORTEX PHASE

For sufficiently weak interactions, the behavior of the system under rotation is dominated by the anharmonicity of the trap, and the many-body wave function is a product of single-particle states describing multiply – or singly-quantized vortex states. Assuming weak interaction ($\sigma a \ll 1$) and weak anharmonicity ($\lambda \ll 1$), we can restrict our attention to a basis of eigenstates of the harmonic potential with zero radial excitations and angular momentum $m\hbar$. (We now set $\hbar = M = \omega = 1$ for convenience. We denote many-body states by capital letters and single-particle states by small letters.) The basis states are

$$\psi_m(\rho, \phi) = \frac{1}{\sqrt{\pi m!}} \tilde{z}^m e^{-|\tilde{z}|^2/2}, \tag{4}$$

where m is a non-negative integer, and $\tilde{z} = \rho e^{i\phi}$. The symmetrized mean-field many-body state with total angular momentum L can then be expanded in this basis as

$$\Psi_{\rm v}(\mathbf{r}_1, \ldots, \mathbf{r}_N) = \prod_{i=1}^{N} \sum_{m=0}^{\infty} \frac{c_m \tilde{z}_i^m}{\sqrt{m!}} \Psi_0, \tag{5}$$

with $\sum_{m=0}^{\infty} m|c_m|^2 = L/N$, and $\sum_{m=0}^{\infty} |c_m|^2 = 1$, where Ψ_0 is the many-body state of the nonrotating cloud,

$$\Psi_0 = \frac{1}{\pi^{N/2}} \exp\left(\sum_{i=1}^{N} -|\tilde{z}_i|^2/2 \right) \Phi_z(z_1, \ldots, z_N). \tag{6}$$

Here, Φ_z is the ground-state many-body wavefunction of the cloud along the z axis. Henceforth, we neglect Φ_z, since it plays no role in our analysis.

The energy of the system in the state $\Psi_{\rm v}$ was calculated in Refs. [10, 12]. Here, we note only certain features related to the trapping potential. If $\mathbf{w}_i = \mathbf{r}_i - \mathbf{R}$ are relative coordinates (with $\mathbf{R}$ the center of mass coordinate), the potential energy can be written as

$$V(\rho_1, \ldots, \rho_N) = \frac{1}{2} \left[\sum_{i=1}^{N} \left({w_i}^2 + \lambda w_i^4 \right) + N R^2 + N\lambda R^4 + 4\lambda R^2 \sum_{i=1}^{N} w_i^2 \right]. \tag{7}$$

In the state $\Psi_{\rm v}$, the first terms, involving w_i, are of order $N\hbar\omega$ and $\lambda N\hbar\omega$; by contrast the last three terms in Eq. (7) are of order $\hbar\omega$ (i.e., unity), $\lambda\hbar\omega/N$, and $\lambda\hbar\omega$, respectively, since $N\langle R^2 \rangle$ is of order unity. Therefore, in

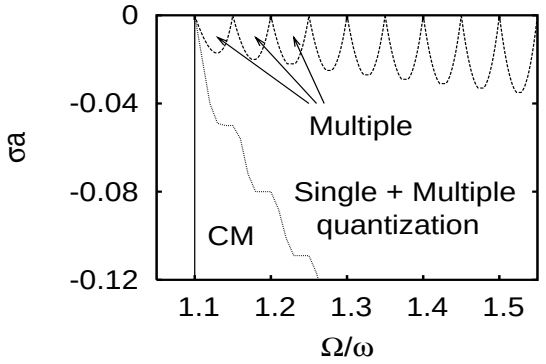


FIG. 2: The phase diagram of a Bose-Einstein condensate trapped in a quadratic-plus-quartic potential in the Ω/ω – σa plane for $\lambda = 0.05$. The vertical line denotes the critical frequency for exciting the center of mass (CM), and the lower dotted line gives the boundary between vortex and center-of-mass motion. To the left of the vertical line, the system does not rotate. The higher dashed line denotes the boundary between pure multiply-quantized vortex states with winding numbers $m = 1$ to 9 and a mixed phase consisting of multiply and singly quantized vortices.

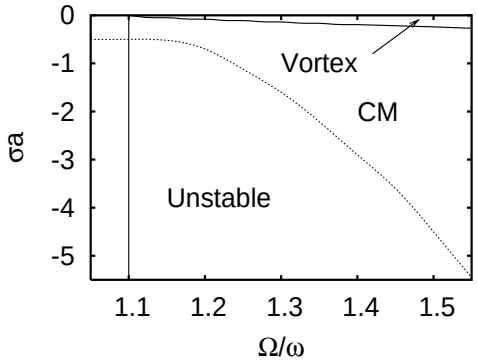


FIG. 3: The same graph as in Fig. 2 for a wider range of values of σa. The higher curve separating the vortex phase and the center of mass phase is the lower curve shown in Fig. 2.

the frame rotating with angular frequency, Ω, the energy per particle of a multiply-quantized vortex state,

$$\Psi_{\rm v}(\mathbf{r}_1,\ldots,\mathbf{r}_N) = \prod_{i=1}^{N} \frac{z_i^m}{\sqrt{m!}} \Psi_0, \tag{8}$$

is

$$\frac{E'_{\rm v}}{N\hbar\omega} = 1 + m\left(1-\frac{\Omega}{\omega}\right) + \frac{\lambda}{2}(m+1)(m+2) + \\ +\sigma a \frac{(2m)!}{2^{2m}(m!)^2}, \tag{9}$$

as in Refs. [10, 12].

As shown in these references, if $\sigma|a|$ exceeds some critical value, the state containing a multiply quantized vortex, described by ψ_m, is unstable against becoming a state of mixed angular momentum of the form

$$\psi = c_{m-1}\psi_{m-1} + c_m\psi_m + c_{m+1}\psi_{m+1}. \tag{10}$$

The dashed curves in Fig. 2 show this phase boundary with $\lambda = 0.05$, for $m = 1$ to 9 from left to right. In each of the regions above the dashed lines, the energy of the gas in the rotating frame is minimized for $|c_m| = 1$, and $|c_{m\pm1}| = 0$.

III. CENTER OF MASS EXCITATION

If the scattering length a is sufficiently negative, we expect the angular momentum to be carried by the center of mass motion [13, 14]. The many-body wavefunction is then,

$$\Psi_{\rm cm}(\mathbf{r}_1,\ldots,\mathbf{r}_N) = \frac{1}{\sqrt{N^L L!}} \left(\sum_{i=1}^{N} z_i\right)^L \Psi_0. \tag{11}$$

where L is non-negative. Calculating the energy per particle of the system in the state $\Psi_{\rm cm}$ in the rotating frame, we find that

$$\frac{E'_{\rm cm}}{N\hbar\omega} = 1 + l\left(1-\frac{\Omega}{\omega}\right) + \frac{\lambda}{2}(l^2+4l+2) + \sigma a, \tag{12}$$

with $l = L/N$. The term $\lambda l^2/2$ comes from the quartic component $\propto R^4$ in Eq. (7), the term $2\lambda l$ results from the component $\lambda\sum_i w_i^4$, while the term λ results from $4\lambda R^2\sum_i w_i^2$. The final term in Eq. (12) is the interaction energy of a non-rotating cloud. Since center of mass motion does not affect the relative coordinates, $\langle V_{\rm int}\rangle$ is unaltered.

Differentiating Eq. (12) with respect to l we find that the critical frequency of rotation of the cloud (for center of mass excitation) is [22],

$$\Omega_c/\omega = 1 + 2\lambda, \tag{13}$$

which is shown, for $\lambda = 0.05$, as the vertical curve in Figs. 2 and 3.

For sufficiently negative interaction strength the energy of $\Psi_{\rm cm}$ becomes smaller than that of $\Psi_{\rm v}$, and we expect a phase transition from the vortex phase investigated in Sec. II to the center of mass state. The overlap between these two states is exponential small in the number of atoms. In the limit of a large number of atoms, this transition is discontinuous in contrast to the transitions examined in Sec. II. In the case of a pure giant vortex given by Eq. (8), for example, the overlap is

$$\langle\Psi_{\rm cm}|\Psi_{\rm v}\rangle = \left(\frac{L!}{N^L(m!)^N}\right)^{1/2} \tag{14}$$

with $L = mN$. In the limit $N \to \infty$,

$$\langle \Psi_{\rm cm} | \Psi_{\rm v} \rangle = (2\pi m)^{1/2} \left(\frac{m^m}{e^m m!} \right)^{N/2} = (2\pi m)^{-N/4}, \quad (15)$$

where last equality applies for $m \gg 1$.

The phase boundary in the $\Omega/\omega - \sigma a$ plane is approximately the line along which $E'_{\rm v} = E'_{\rm cm}$, given by Eqs. (9) and (12). This result is shown as the lower (higher) curve in Fig. 2 (Fig. 3). In fact, the true phase boundary lies even lower since the energy for the single-particle mixed states of the form $\psi = \cdots c_{m-1}\psi_{m-1} + c_m\psi_m + c_{m+1}\psi_{m+1} \cdots$ is necessarily smaller than that for $\psi = \psi_m$ in this region.

IV. UNSTABLE PHASE

Sufficiently large attractive interactions render the cloud unable to support itself, and a dense atomic state results. In a nonrotating system, this instability occurs when $\sigma|a|$ is on the order of unity [16, 17]. As we show below, in a rotating cloud this value is even more negative because of the kinetic energy of the rotational motion [23].

To calculate the phase boundary, we start with the energy in the rotating frame in the state $\Psi_{\rm cm}$, Eq. (12), but regard the corresponding oscillator length as a variational parameter. We previously assumed that the oscillator length is fixed and given by $(\hbar/NM\omega)^{1/2}$. Here, we perform the same calculation assuming that the oscillator length is $\beta(\hbar/NM\omega)^{1/2}$, where β is real and positive. The result is

$$\frac{E'_{\rm cm}}{N\hbar\omega} = \frac{1+l}{2}(\beta^2 + \frac{1}{\beta^2}) - l\frac{\Omega}{\omega} + \frac{\lambda}{2}[l^2\beta^4 + (4l+2)\beta^2] + \frac{\sigma a}{\beta^2}. \quad (16)$$

For a non-rotating cloud, the value of β that minimizes the energy is

$$\beta_0 = \left(\frac{1+2\sigma a}{1+2\lambda} \right)^{1/4}, \quad (17)$$

which implies that the critical value for collapse is $\sigma a = -1/2$.

Differentiating $E'_{\rm cm}$ with respect to l we obtain

$$l = \left[\frac{\Omega}{\omega} - \frac{1}{2}\left(\beta^2 + \frac{1}{\beta^2} \right) - 2\lambda\beta^2 \right] \frac{1}{\lambda\beta^4}, \quad (18)$$

so that the critical frequency for center of mass excitation is

$$\frac{\Omega_c}{\omega} = \frac{1}{2}\left(\beta^2 + \frac{1}{\beta^2} \right) + 2\lambda\beta^2. \quad (19)$$

This expression reduces to Eq. (13) when $\beta \to 1$ in the limit of weak interactions, $\sigma a \ll 1$ and $\lambda \ll 1$. The point where $E'_{\rm cm}$, expressed in terms of β, Ω/ω, σa, and λ, ceases to have a local minimum as function of β, signals the collapse of the cloud. The result for $\lambda = 0.05$ and varying Ω/ω and σa is shown in the lower line of Fig. 3.

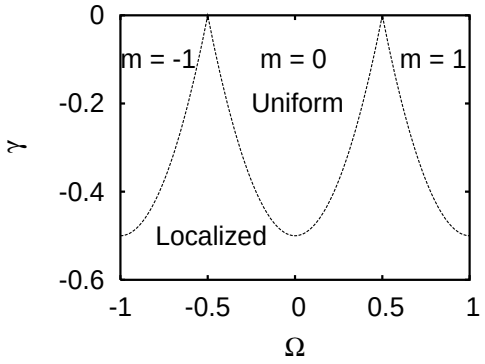


FIG. 4: The phase diagram of an effectively attractive Bose-Einstein condensate confined in a toroidal trap, from Ref. [24]. Here γ is the ratio between the interaction energy and the kinetic energy, corresponding to σa in the present problem, and Ω is the dimensionless rotational frequency of the torus. The function $\gamma(\Omega)$ is periodic.

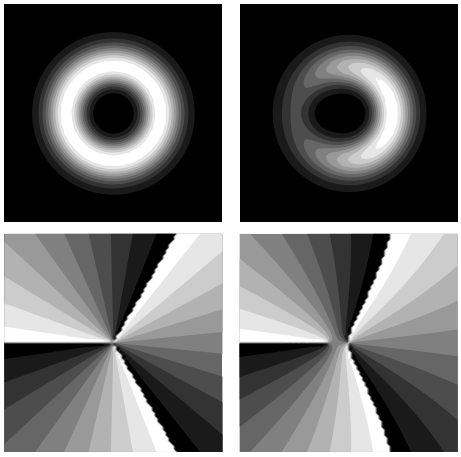


FIG. 5: Equipotential plots of the density (higher) and phase (lower) of the condensate in the state of the form of Eq. (10) for $m = 3$. In the left graphs $c_2 = c_4 = 0$, while in the right ones all c_m are nonzero. The left graphs correspond to the uniform phase of the one-dimensional problem, while the right ones correspond to the localized phase. The axes extend from $-4d_0$ up to $4d_0$.

V. FEATURES OF THE PHASE BOUNDARY

The calculated phase diagram of Fig. 2 is universal [10, 12] in the sense that the same graph would be obtained for $\lambda' = \alpha\lambda$ by rescaling the axes by α, i.e., $(1 - \Omega/\omega) \to \alpha(1 - \Omega/\omega)$ and $\sigma a \to \alpha\sigma a$. Further, the

dashed line indicating the phase boundary between pure multiple quantization and the mixed phase is exact in the limit of small λ and $\sigma|a|$ [10, 12]. In the phases of multiple quantization, the energy in the rotating frame is minimized (i.e., the energy is an extremum and its second derivative with respect to admixtures of other states is always positive). Thus, even though the effective interaction is attractive in this system, the vortices of the driven system are stable against small perturbations. Furthermore, as one decreases Ω/ω crossing the segments of fixed m, there is a continuous path along which the energy decreases towards the absolute minimum of the energy (in the lab frame). This implies that there can be no persistent currents, in agreement with the toy model presented in Sec. VI of Ref. [19].

The higher phase boundary in Fig. 2 closely resembles that of a rotating Bose-Einstein condensate confined in a one-dimensional toroidal trap, with an effective attractive interaction between the atoms. This system was investigated in Refs. [21, 24]; its phase diagram is shown in Fig. 4. In this one-dimensional problem the instability of states of the form $\phi_m = e^{im\phi}/\sqrt{2\pi}$ is actually towards the combination $c_{m-1}\phi_{m-1} + c_m\phi_m + c_{m+1}\phi_{m+1}$, which is the one-dimensional analogue of our problem. [See Eq. (10).] The reason for this resemblance is the form of the effective potential felt by the atoms,

$$V_{\rm eff} = V - M\Omega^2\rho^2/2, \tag{20}$$

which has a mexican-hat shape for $\Omega > \omega$. We identify the phase of pure multiple quantization as the uniform state of the one-dimensional problem and the other two phases as the localized state of the one-dimensional case. References [22] exclude the possibility of a state of the form of Eq. (10). However, at least for the parameter range considered here close to the phase boundary, there is also a mixed phase for which the order parameter has the form of Eq. (10).

When $c_{m-1} = c_{m+1} = 0$, these states describe multiply-quantized vortices of winding number m, and the density is homogeneous, as shown on the left upper graph of Fig. 5 (for $m = 3$.) We see in the lower left graph a triply quantized vortex at the origin. On the other hand, when c_{m-1} and c_{m+1} are nonzero, these states describe a combination of a multiply-quantized vortex ($m = 2$) at the center of the cloud with winding number $m - 1$, here 2 in the lower right figure, one singly-quantized vortex just to left close to the origin, and another not shown, much further from the center, where the density is very low. As shown in the upper right graph of Fig. 5 (for $m = 3$), the density is now inhomogeneous (and resembles that corresponding to the center-of-mass phase). This is an energetically favourable configuration because the effective atom-atom attraction prefers the inhomogeneity around the minimum of the effective potential $V_{\rm eff}$. The reason why the minima in the phase boundary of Fig. 2 decrease with increasing Ω/ω (as opposed to the one-dimensional case) is that the radius of the toroidal trap corresponding to $V_{\rm eff}$ increases with Ω/ω.

We also note that with increasing Ω, at fixed σa, center of mass excitation always occurs before quantized vortices are formed. The states $\Psi_{\rm cm}$ and $\Psi_{\rm v}$ cannot be connected by low-order application of any single-particle operator because of their small overlap, as noted above. Thus, even in the region where $\Psi_{\rm v}$ has a lower energy than $\Psi_{\rm cm}$, the system can remain in $\Psi_{\rm cm}$ for times which can be very long (i.e., that scale at least linearly with the number of atoms N.) The calculation of this time scale remains a difficult open question. On the other hand, if one first rotates the gas above the condensation temperature and then cools down, the system will end up in the phases shown in Fig. 2.

VI. SUMMARY

We have calculated the phase diagram for a rotating Bose-Einstein condensate in a quadratic-plus-quartic potential when the effective interaction between the atoms is effectively attractive. For very weak interactions there is a phase of (pure) multiply quantized vortices. In this phase the energy of the gas in the rotating frame is minimized and the vortex states are stable against weak perturbations. For somewhat more attractive interactions, there is a mixed phase of single and multiple quantization. For even more attractive interactions, the system carries its angular momentum via center of mass excitation. Finally for even stronger attraction, the cloud cannot support itself and collapses to a dense atomic state.

Author GMK wishes to thank Emil Lundh and Ben Mottelson for useful discussions.

[1] C. J. Pethick and H. Smith, *Bose-Einstein Condensation in Dilute Gases*, Cambridge Univ. Press (Cambridge, 2002).
[2] D. A. Butts and D. S. Rokhsar, Nature **397**, 327 (1999).
[3] G. M. Kavoulakis, B. Mottelson, and C. J. Pethick, Phys. Rev. A **62**, 063605 (2000).
[4] V. Bretin, S. Stock, Y. Seurin, and J. Dalibard, Phys. Rev. Lett. **92**, 050403 (2004).
[5] E. Lundh, Phys. Rev. A **65**, 043604 (2002).
[6] A. L. Fetter, Phys. Rev. A **64**, 063608 (2001).
[7] K. Kasamatsu, M. Tsubota, and M. Ueda, Phys. Rev. A **66**, 053606 (2002).
[8] G. M. Kavoulakis and G. Baym, New J. Phys. **5**, 51.1 (2003).
[9] A. Aftalion and I. Danaila, Rev. A **69**, 033608 (2004).
[10] A. D. Jackson and G. M. Kavoulakis, to appear in Phys.

Rev. A.
[11] U. R. Fischer and G. Baym, Phys. Rev. Lett. **90**, 140402 (2003).
[12] A. D. Jackson, G. M. Kavoulakis, and E. Lundh, Phys. Rev. A **69**, 053619 (2004).
[13] N. K. Wilkin, J. M. F. Gunn, and R. A. Smith, Phys. Rev. Lett. **80**, 2265 (1998).
[14] B. Mottelson, Phys. Rev. Lett. **83**, 2695 (1999).
[15] C. J. Pethick and L. Pitaevskii, Phys. Rev. A **62**, 033609 (2000).
[16] G. Baym and C. J. Pethick, Phys. Rev. Lett. **76**, 6 (1996).
[17] M. Ueda and A. J. Leggett, Phys. Rev. Lett. **80**, 1576 (1998).
[18] E. Mueller and G. Baym, Phys. Rev. A **62**, 053605 (2000), and references therein.
[19] A. J. Leggett, Rev. Mod. Phys. **73**, 307 (2001).
[20] H. Saito and M. Ueda, cond-mat/0306319;
[21] R. Kanamoto, H. Saito, and M. Ueda, Phys. Rev. A **68**, 043619 (2003).
[22] E. Lundh, A. Collin, and K.-A. Suominen, Phys. Rev. Lett. **92**, 070401 (2004); e-print cond-mat/0403326.
[23] As first pointed out by B. Mottelson, private communication.
[24] G. M. Kavoulakis, Phys. Rev. A **69**, 023613 (2004).